Soil Behavior of Wheels with Grousers for Planetary Rovers

Scott Moreland
Carnegie Mellon University
5000 Forbes Ave
Pittsburgh, PA 15213
412-592-4455
Scott.J.Moreland@cmu.edu

Krzysztof Skonieczny
Carnegie Mellon University
5000 Forbes Ave
Pittsburgh, PA 15213
KSkoniec@andrew.cmu.edu

Hiroaki Inotsume
Dept. of Aerospace Engineering, Tohoku University
Aoba 6-6-01, Sendai, 980-8579, Japan
Inotsume@astro.mech.tohoku.ac.jp

David Wettergreen
Carnegie Mellon University
5000 Forbes Ave
Pittsburgh, PA 15213

***Abstract*—The performance of wheels operating in loose granular material for the application of planetary vehicles is well researched but little effort has been made to study the soil shearing which governs traction. Net traction measurements and application of energy metrics have been solely relied upon to investigate performance but lack the ability to evaluate or describe soil-wheel interaction leading to thrust and resistances. The complexity of rim and grouser interaction with the ground has also prevented adequate models from being formulated. This work relies on empirical data gathered in attempt to study the effects of rim surface on soil shearing and ultimately how this governs traction. A novel experimentation and analysis technique was developed to enable investigation of terramechanics fundamentals in great detail. This technique, the Shear Interface Imaging Analysis Tool, is utilized to provide visualization and analysis capability of soil motion at and below the wheel-soil interface. Analysis of the resulting displacement field identifies clusters of soil motion and shear interfaces. Complexities in soil flow patterns greatly affect soil structure below the wheel and the resulting tractive capability. Grouser parameter variations, spacing and height, are studied for a rigid wheel. The results of soil shear interface analysis for wheels with grousers are presented. The processes of thrust and resistances are investigated and behavior characterized for grousered wheels.**

TABLE OF CONTENTS

1. INTRODUCTION

The use of features on the rim of wheels, such as grousers, has been relied upon for increasing traction of mobility platforms in a wide range of applications. Performance measurements for use in loose, granular soil have shown tractive gains for many implementations of these features [1] but little empirical data exists on the mechanisms and processes present in the soil that contribute to the increases in mobility capability. Additionally, there exists no theory that is well supported pertaining to the soil failure characteristics created by wheel operations with grousers. This has lead to a generally poorly understood but commonly implemented design feature of wheels for planetary rovers and other systems traversing loose, granular soil. Of theory that exists, no direct empirical evidence has been offered to validate the soil failure that governs how thrust is generated by grousers. The general lack of knowledge has created a "rule of thumb" type approach to the use of grousers when wheel design is approached.

To date, the investigation of the function of grousers for planetary vehicles has taken the approach of relying solely on performance measurements. Net traction, sinkage, slippage, wheel torques, power and reaction forces are typically measured during single wheel testing over a wide range of parameter changes, such as grouser spacing or height. Trends in the data are used to determine optimal parameter combination and conclusions sometimes inferred from these results. This approach is suitable for determining the response and performance of specific designs but provides limited information on the actual mechanisms and processes occurring in the soil that govern traction. Therefore, little knowledge can be gained in understanding how grousers function in general and how they should be implemented in design and vehicle operation.

The work discussed in this paper follows an approach of studying the soil shearing behavior of wheels with grousers with the objective of learning the mechanics and processes in effort to discover what leads to increased performance when grousers are employed. The approach was to experimentally characterize soil shearing behavior over a range of parameter changes in addition to performance measurements resulting from reaction forces. A novel soil shearing analysis technique for wheel terramechanic investigation was utilized and was the primary tool for this study. This method, called Shear Interface Imaging Analysis [2], allowed for empirical evidence to be collected in support of new theory of grousered wheel operation introduced in this study.

978-1-4577-0557-1/12/$26.00 ©2012 IEEE

This paper first describes the soil shearing analysis technique (Section 2) relied upon as primary source of data for results. The experimental approach followed for investigation of grousered wheels in this work is explained in Section 3. Results of experimentation and theories of grouser wheel-soil behavior are introduced in Section 4.

2. WHEEL SOIL SHEARING ANALYSIS

Methods available utilizing common terramechanics approaches do not achieve high fidelity results and are not appropriate for lightweight vehicles in loose, granular materials. Difficulties are also presented with the analysis of most wheel designs due to the complexities of interface interaction of the rim with the soil below.

The design of traction devices such as wheels for planetary rovers rarely involves the detailed analysis of the soil shearing and failure patterns. The stress applied to the soil mass is not only the result of external loading but also directly affected by the operation of the wheel. The application of torque during wheel rotation creates unique shearing patterns that vary widely in ability to support shear loading. The 'shear interface' are failure planes that develop in the soil below the region of interaction with the rim. Shear interfaces can indicate the soil failure type, location, size and strength. Geometry of the rim, presence of grousers, wheel stiffness, contact shape and many other properties have large effects on the shear interface during operation of a wheel. The performance of a traction device in loose, granular soil is ultimately governed by the soil properties and the shear failure that occurs. The shearing processes, shear failure types and flows determine how large a reaction load can be obtained to generate thrust and the type of motion resistances and their magnitude present leading to the net traction available. The experimental apparatus constructed to analyze the soil shearing below a wheel consists of a glass-walled soil bin filled with regolith simulant, a traction device specimen, an actuated horizontal axis of motion (Figure 1) and a high-speed camera. The wheel module (Figure 2) of the imaging test bed is position or velocity controlled in coordination with the horizontal axis to create a commanded, constant slip as the wheel travels forward. A linear rail allows the wheel to translate freely in the vertical direction allowing for natural sinkage to occur. This also allows for the transmission of a payload of dead weights to be applied to the wheel. A 6-d.o.f. force/torque sensor is incorporated to measure the reaction loads, specifically in the horizontal (travel) direction as a result of traction generated. Sinkage is also measured via an optical encoder affixed to the vertical free linear axis. All telemetry; wheel angular velocity, travel velocity, slip, sinkage, load and power are logged simultaneously at 6.25Hz or higher.

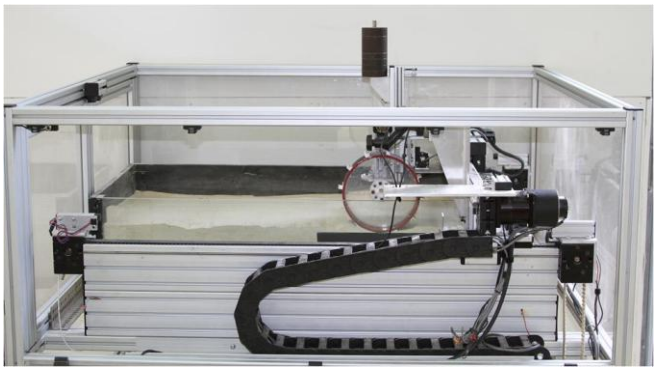

Fig 1: *Single Wheel Soil Imaging Testbed. Wheel travels from left to right with controlled slip along a belt-driven linear axis.*

The wheel for all shear imaging analysis experiments is pressed against a sheet of tempered glass that extends the depth of the soil bin. Of importance is the use of a wheel of half the width of the actual specimen of interest and the application of half the payload weight. The boundary condition of the full-width wheel mid width (center) in the plane perpendicular to the rotation axis must be maintained during the soil shear imaging experiments. This boundary condition of zero shear stress along the plane of symmetry is equivalent to the half-width wheel against the glass provided that the soil particle-glass interface is sufficiently low friction (ideally zero). This is achieved by the use of tempered glass with a high hardness surface and by the low pressure of the soil particle against the glass wall.

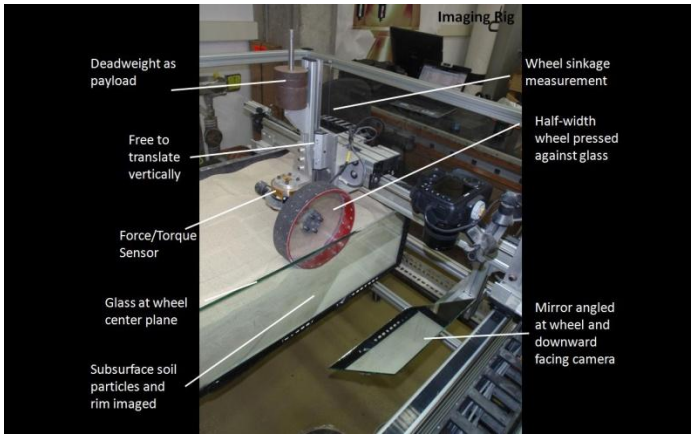

Fig 2: *Wheel module, carraige (travel axis) and glass-walled soil bin. A 31x22cm coss-section of soil below the wheel is imaged with a highspeed camera.*

The shearing analysis requires the ability to track soil motion. A digital SLR camera with a 50mm macro lens is used to image the wheel-soil interface, logging frames locally on a laptop simultaneously with the rest of the telemetry previously discussed. A frame rate of 8 frames-per-second is used and is sufficiently fast for the slow speeds of wheel travel applied. The camera is mounted

perpendicular to the soil bin glass wall and travels with the wheel in the horizontal direction as the carriage moves. For most wheel specimens (23cm to 50cm) a 31cm wide by 22cm high patch of soil is framed and able to capture the complete shear interface produced by the wheel in the regolith simulants used. External halogen flood lights at a high angle normal to the glass are utilized to illuminate the soil particles.

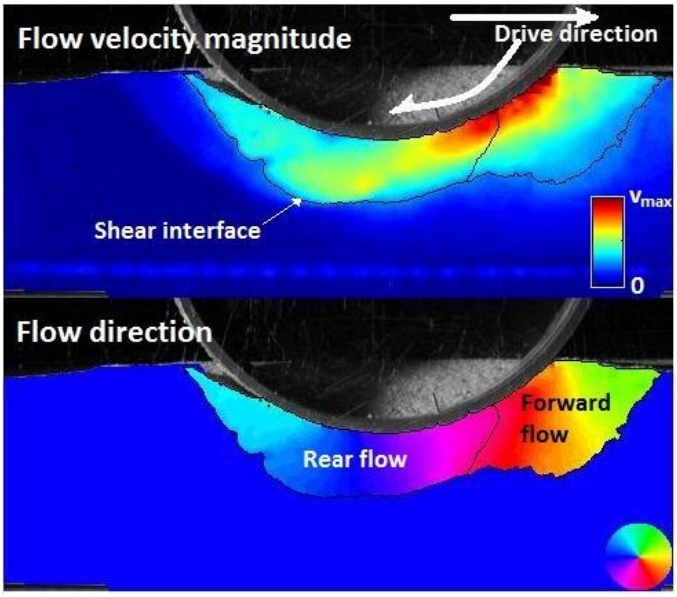

Fig 3: *Shear Interface Imaging plots. Plots show soil flow magnitude (top) and direction (bottom). Magnitude is plotted from dark blue (stationary soil) to red (representing the soil flowing at highest speed). Direction (within the shear interface) is plotted representing 360^o as shown in the legend. This sample output of the process, showing soil flow magnitude, shear interface between significant and insignificant flow, soil flow direction (within region of significant flow), and boundary between forward and rear flow.*

Image processing comprises of optical flow and clustering techniques. The optical flow algorithm [3] tracks displacement of soil regions relative to a prior frame and calculates a motion vector at each pixel. Initial clustering separates each image into "soil" and "not soil" regions. Additional processing and output is continued only for "soil" regions.

The magnitude of flow at each pixel of the soil regions is calculated from the optical flow vector fields. Soil flow is clustered into "significant" and "insignificant" magnitudes of motion. No explicit threshold is used to demarcate these clusters, but rather automatically adaptive clustering is used. The shear interface is derived from the boundary between significant and insignificant motions.

Soil flow direction is calculated from the optical flow vector fields, for soil regions exhibiting significant soil flow. Soil flow in any direction (360 degrees) is visualized, and an additional boundary is identified at points where the soil transitions between forward and rear flow.

The shear interface is indicative of the soil failure process and type. Analysis of this and the flows present within the soil can aid with design of traction devices and study of terramechnic fundamentals. Figure 3 shows the processed results of a single wheel shear interace imaging analysis experiment. The Flow Velocity Magnitude and Flow Direction plots are used to analyze the wheel. These plots show processes typically present within the soil of a wheel operating in loose, cohensioless soil.

The flow velocity field plot uses the optical flow velocity field measured between image pairs and clustering methods for classification to display the soil flow speed. These plots (Figure 3, top) scale from dark blue (stationary soil) to red (representing the soil flowing at maximum speed,V_{max}). This type of plot allows for the evaluation of the soil flow due to shearing. The shear interface is a key indicator of the means by which the wheel produces traction. This term, for purposes of this study, is defined as the region (line or band like in shape) where soil transitions from measured shear displacement (flowing) to near static (not flowing).

The Flow Direction plot (Fig. 3, bottom) displays the direction of soil particle shearing as measured by the flow velocity field. The multi-colored wheel is the legend that maps color to direction with respect to the wheel coordinate frame. ‘Dark blue‘ indicates soil particles moving completely horizontal in the left hand direction, opposite the direction of wheel travel. The direction of shearing aids in determining what type of soil failure process occurs, design feature that may contribute to the failure and the identification of mulitple flows, such as resistive types at the wheel front. The seperation of two flows (Figure 3, bottom), as detected by the developed analysis software, allows for the identification of forward flows and the measurement of the location of point of maximum shear stress along the rim. This occurs at the intersection of the wheel rim and flow separation point.

3. GROUSERED WHEEL EXPERIMENTATION

The objective of this papers study was to characterize the soil shearing processes occurring during operation of a rigid wheel with grousers in hope of learning why net thrust is affected by these features and how they should be implemented. The approach followed five steps.

1) Conduct a wide survey of grouser parameters (spacing and height) up to reasonable extremes to investigate the shearing processes and traction performance.

2) Identify trends in external reaction loads such as a ‘knee’ in traction-spacing curve.

3) Fill in critical data points near changes in loads trends so changes in soil shearing can be observed about these points (knees, plateaus, etc).

4) Develop theory for motion resistances, sinkage or thrust based off observed soil shearing.

5) Check theory applies to all grouser configurations tested and add more configurations if needed.

Important aspects of the configuration of the hardware for experimentation includes wheel diameter, wheel width, slip ratio, soil simulant, soil simulant preparation, wheel payload (normal load), wheel rotational speed, and method of applying travel resistance. The single wheel imaging rig shown in Fig. 1 was utilized for this study. This apparatus was utilized in a controlled slip mode for all experiments. Data was collected at 20% wheel slip for all grouser parameter combinations, however full slip curves (5% to 60% slip at 5% intervals) were generated for some combinations to assess soil shearing through many operating regimes. The wheel tangential rim speed was held constant at an equivalent no slip ground speed of 2cm/s, while the carriage speed was controlled to vary slip ratio. A single wheel rim size, with dimensions of 23cm diameter by 5.72cm wide, was used for the experiments. This specimen used for soil imaging as explained in Section 2, is equivalent to a 11.4cm wide wheel that is twice the width and carrying twice the payload (however, same ground pressure). A 10kg payload was applied to the wheel creating an average ground pressure of 22kPa (by measuring contact area at 20% slip and no grousers). This payload and ground pressure is relevant to planetary vehicles, such as the NASA Mars Exploration Rovers. The single wheel imaging test bed was prepared with GRC-1 lunar soil simulant [4] before each test run. The soil is loosened to a state of lowest relative density and slightly compacted by use of a drop tamper method to produce repeatable soil properties. Shear strength measurements were taken after each soil preparation to verify consistent strength properties. A torsional shear strength tester modified for constant normal pressure control was used [5].

The single wheel imaging rig logged soil response, external reaction loads and actuator energy values. Soil response and reaction loads were the primary data source investigated for this study. A list of the measurement types is shown below.

A) Soil Response

- Shear interface imaging analysis tracking subsurface soil flow – Optical measurements using high-speed digital camera and optical flow processing
- Wheel Sinkage – linear encoder measuring vertical wheel travel

B) External Reaction Loads

- All force and torques – net thrust (drawbar pull), actuator torques, etc. using 6-degree of freedom force-torque sensor (ATI Delta F/T model)

C) Energy - Current/Power

- Wheel energy efficiency metrics – motor controller voltages and current measured

An approach of surveying the operation of a wide range of grouser height and spacing combinations was followed to investigate soil shearing behavior of a wheel specimen. Shown in Table 1 is the height and number of grousers mounted to the wheel for each experiment. It should be noted that at least three repeats were conducted for each configuration and values of metrics were averaged.

Drawbar pull is a performance metrics utilized in this study. The net thrust, often referred to as drawbar pull [6][7], is the most widely used metric for traction. It is evaluated at 20% slip in this work unless otherwise stated and is normalized by wheel payload.

Table 1 – Experiment Matrix

t=tested, p=shear interface analysis processed, x=not tested

# Grousers **Height**	6	12	16	24	32	48
13mm	t,p	t,p	t,p	t,p	x	t,p
10mm	t	t,p	t,p	t,p	x	t,p
6.4mm	x	t	x	t	t	t
0 (no lug)	t,p *w/ sand paper rim at root diameter					

Soil shear interface imaging analysis relies on still image data produced by the digital camera. Results for the experiments indicated in Table 1 are provided in the next section.

4. RESULTS

The performance plot of figure 4 shows a significant increase in drawbar pull for many configurations of the grousers with a trend of increasing traction with larger height and smaller spacing. There is also a plateau in the trend as number of grousers increase. It is desirable to identify the physical phenomena of the wheel interaction of the soil and the resulting shearing that results in this these trends. Shear interface analysis sheds some light onto what processes may be occurring.

The periodic response of the reaction loads (drawbar pull versus time shown in figure 5, soil shearing in figure 6) is a key observation. In addition to this, there is a major peak in the series for each grouser entering the soil for all spacing tested (figure 6). This is an important realization as it shows

that each grouser has an individual effect on drawbar and may not share thrust loads. This is consistent with later observations that show there may be little effect on thrust due to grousers.

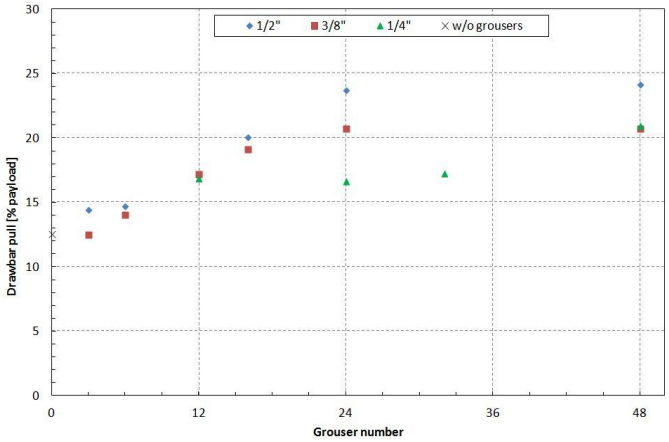

Fig 4: *Drawbar pull results for 23cm diameter, rigid wheel with grousers at six spacing's and four heights. This are evaluated at 20% slip and averaged over the steady state portion (although highly periodic) of response. The use of grousers show significant increase in drawbar for some configurations and also exhibit a plateau in performance.*

There is also an observable decrease in variation (amplitude of periodic curve) of the drawbar pull as a function of time as the spacing decreases. It can also be noted that the absolute value of the peaks do not vary as much as the troughs as grouser spacing decrease. Although only two spacing's are shown in figure 5, this trend is maintained for all five spacing's tested for a given height. Theory introduced later may explain why the lower limits of the troughs are similar to the value of drawbar pull without grousers.

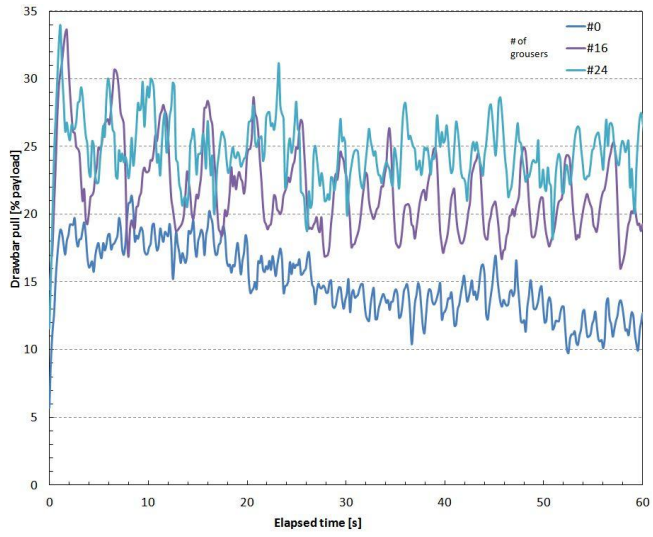

Fig 5: *The drawbar pull is shown to be highly periodic for wheels with grousers. For these wheels, major period is observed to be proportional to grouser spacing. For a constant drawbar pull test, the slip becomes periodic.*

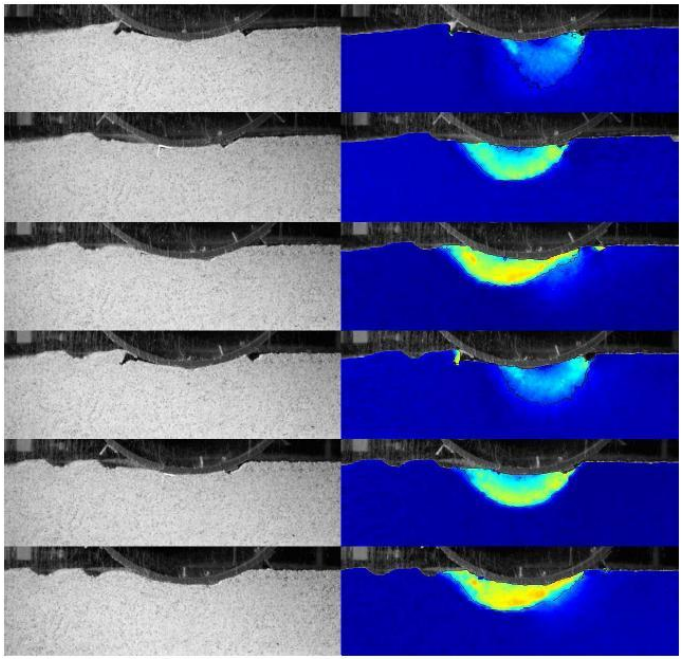

Fig 6: *Timelapse images of soil sheared by a wheel with grousers over two cycles (grousers) (flow magnitude plot).The shearing is dominated by the leading lug, and exhibits distinct periodic soil motion as each new lug rotates into the soil. This occurs for even small grouser spacing's however the magnitude of soil shearing is lowered. Wheel travel is left to right.*

Periodic soil shearing is evident from the test results shown in figure 6. The cyclic soil shearing shows that there is either poor load sharing amongst grousers when generating thrust or periodic effects on motion resistance due to each grouser. Further investigation supports the latter.

The traction performance of the wheel without grousers (sand paper rim) and the wheel with 48 grousers at 13mm height act as extremes of the configurations and drawbar pull performance (Figure 5). Studying these two cases leads to an important realization. The soil displacement behavior of the grouserless wheel (Figure 7) and the 48 grouser wheel (Figure 8) exhibit very different behavior at the leading edge of the wheels. The Figure 7 direction plot, no grousers, shows a yellow patch of soil in front of the wheel that moves in a horizontal direction forward (low magnitude and within compaction regime). This is evidence of a significant motion resistance that would be reacted against the rim as soil is pushed forward and compacted downwards. This observed motion resistance would reduce the drawbar pull of the wheel. The wheel with highest drawbar pulled tested (48 grousers at 0.5" height) however does not show any evidence of a motion resistance such as compaction resistance. Additionally, a low resistance large diameter wheel did not have any observable forward flow (Figure 10). For rigid wheels operating at ground pressures and in soils relevant to planetary surface vehicles, compaction resistance is usually in the range of 30% to 50% of available thrust, thus drastically reducing drawbar pull available (net

thrust). It is reasonable to conclude from this observation that grousers can be implemented to significantly reduce compaction resistance and lead to higher drawbar pull. Then net traction can be expressed as thrust minus resistances. An increase in drawbar could also arise from an increase in thrust. Observations of soil shearing may also suggest whether the grousers provide additional thrust.

There are two distinct regions with different soil behavior below the rolling wheel. The region of forward flow under the rim (indicated in Figure 3) undergoes compaction. As this soil is in contact in front of the wheel dead center, the downward compaction of the soil can create resistant forces in the radial direction with a component of this in the rearward direction. The soil of the rear flow contributes to thrust. The general shape and size of the shear interface is an indicator of differences in thrust of the grousered and non-grousered wheels.

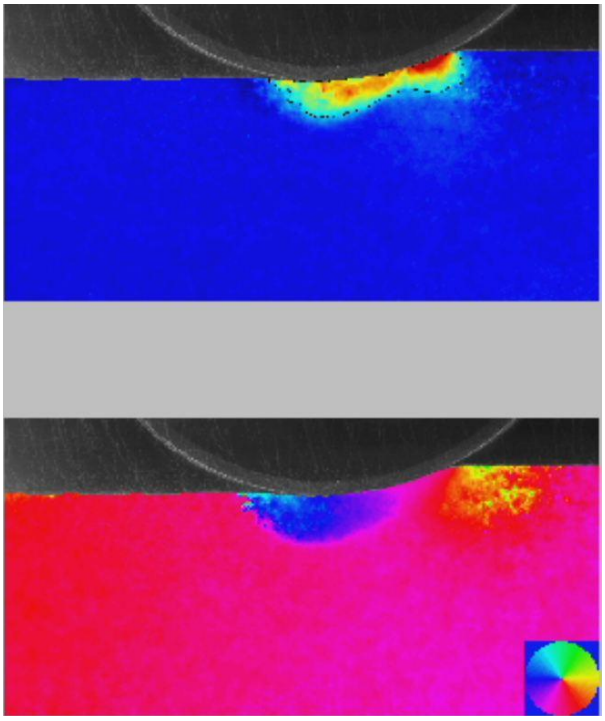

Fig 7: *Plots shown are particle velocity magnitude (top) and direction (bottom). Unlike figure 3, there is no threshold on the direction plot of figure 7and 8. The 'pink' soil in the bulk direction plot is stationary (except directly under the wheel). Compaction of soil in forward direction (yellow) is visible in front of leading edge (right) of wheel. This is evidence of forward motion resistance.*

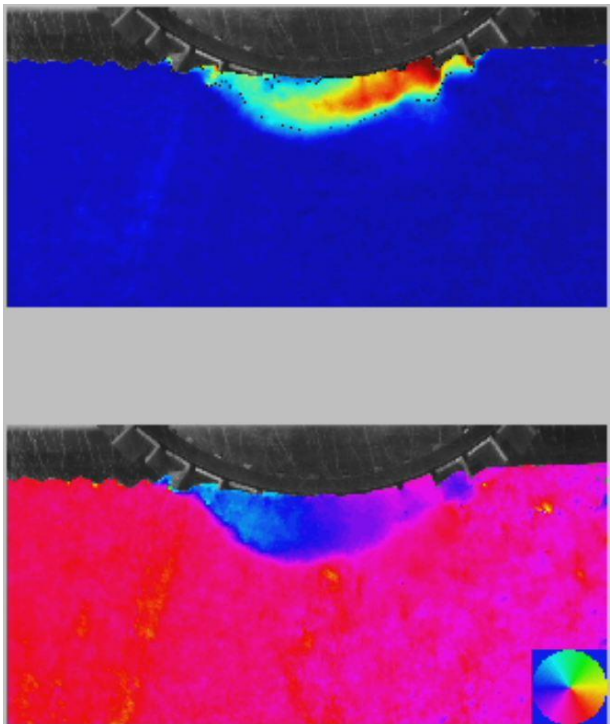

Fig 8: *For a high drawbar grousered wheel (48lugs at 0.5" height), no observable evidence of forward compaction exists at the leading edge of the wheel. Therefore, little motion resistance should be present. Motion left to right.*

The rear shear interface of grousered and non-grousered wheels are quite similar. If it is assumed that in the rear flow region, the grousers are full of compacted soil, it will act like a wheel of larger diameter (only for the rear flow region, not front entrance area). With this assumption, the length, depth and shape of the shear interfaces of the two wheels are remarkably similar. If the magnitude of shearing and the soil density are similar, than the strength along the shear interface should be similar. The absolute shearing magnitude of the two wheels was measured to be similar using absolute particle velocity plots. Additionally, a reasonable assumption can be made that the soil density (as GRC-1 is not highly compactable) in the rear flow region behind the wheel center would have undergone similar compaction do to wheel payload. For these reasons, the soil strength can be assumed to be similar. As the shear interface shape/size and soil strength are similar, it is reasonable to conclude that the thrust component of the drawbar pull are of similar value for both grousered and non-grousered wheels. Differences in thrust due to drastically different shear interfaces can cause high changes in thrust [8], however the failure modes are of the same type for both shear interface observed. As such, it is theorized that the gain in drawbar pull due to implementation of grousers arises solely from the reduction of compaction resistance.

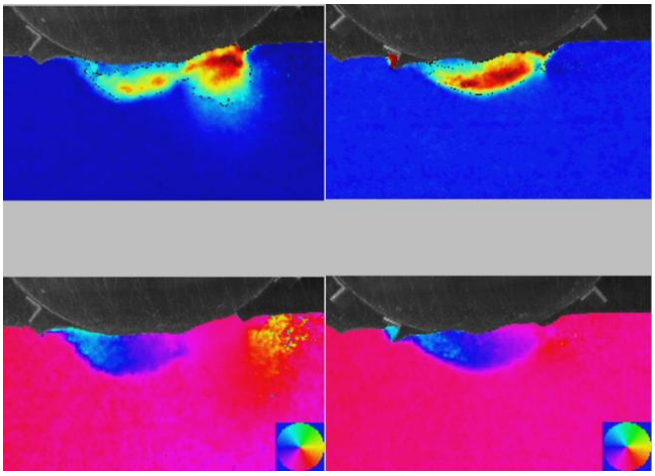

Fig 9: *Wheel with widely spaced grousers (16 grousers for displayed specimen) displays periodic forward flow. Movement of soil in front of the wheel is observed to occur when rim begins to compact soil that is not directed under the wheel by the grousers. Loss of drawbar pull is measured during these periodic processes.*

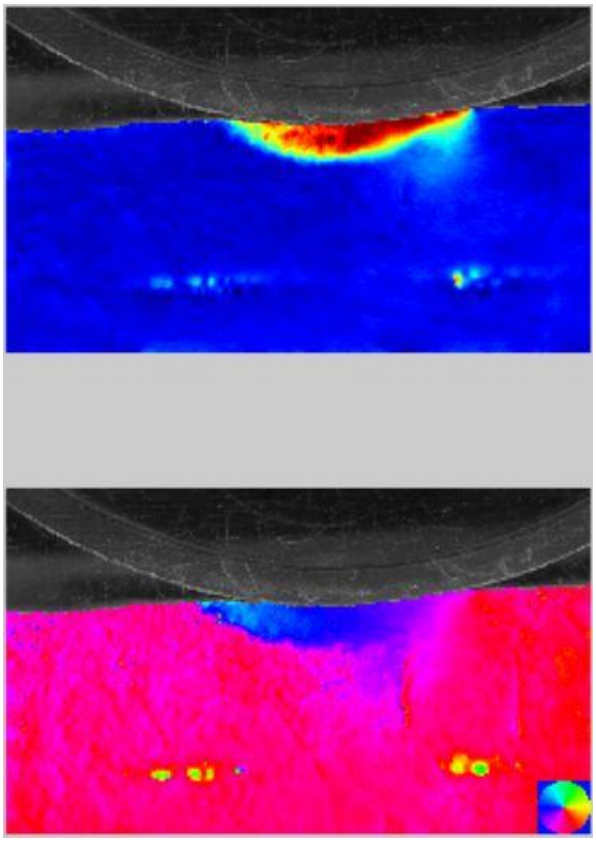

Fig 10: *Large diameter wheel (41cm DIAM above) does not display observable forward flow or forward compaction. This is expected for a large diameter wheel operating at low sinkage, resulting in little motion resistance*

5. CONCLUSION

Shear interface imaging provided new information with respect to the shearing behavior of soils as a result of wheel operation with grousers. Single wheels test load cell measurements shows that wheels with grousers can be configured to increase drawbar pull. Compaction in the forward flow region in front of the contact area was not observed for wheels with grouser that generate high drawbar. Additionally, the shear interface of the region associated with generating thrust is similar for wheels with and without grousers. It is reasonable to conclude that increases in drawbar pull of wheels with grousers arises solely from the decrease in compaction resistance. The increase in drawbar pull most likely is due to a decrease in motion resistance, not from an increase in thrust. This work contributes a new theory of the operation of wheel grousers which should be further studied to generate results beyond these preliminary findings. Below are a recap of major observations and conclusions as a result of this study.

- Single wheel test load cell measurements shows that wheels with grousers can be configured to increase drawbar pull.
- Compaction in the forward flow region in front of the contact area was not observed for wheels with grousers that generate high drawbar.
- Additionally, the shear interface of the region associated with generating thrust is similar for wheels with and without grousers. It is reasonable to conclude that increases in drawbar pull of wheels with grousers arises primarily from the decrease in compaction resistance.
- The increase in drawbar pull most likely is due to a decrease in motion resistance, not from an increase in thrust.
- Reduction of forward soil motion for grousers wheels correlated with grouser spacing/height that excavated at the leading edge enough to drastically lower the contact angle (rim first contacts soil much further under wheel)

6. ACKNOWLEDGEMENTS

This research was supported by NASA under grants NNX07AE30G, Colin Creager (GRC) and the JPL SURP program (1220-DRDF-104425), Gregory Davis.

REFERENCES

[1] **Ding, L; Gao, H; Z, Deng; Yoshida, K.; Nagatani, K.;** 2009. *Slip ratio for lugged wheel of planetary rover in deformable soil: definition and estimation.* IROS 2009, St. Louis, MO

[2] **Moreland, S., Skonieczny, K., Wettergreen, D., Asnani, V., Creager,** 2011. *Soil Motion Analysis System for Examining Wheel-Soil Shearing.* 17th International Conference for the Society of Terrain-Vehicle Systems, Blacksburg, VA

[3] **Black, M. J. & Anandan, P.** 1996. *The robust estimation of multiple motions: Parametric and piecewise-smooth flow fields,* CVIU, 63(1), pp. 75-104.

[4] O**ravec, H., Asnani, V., & Zeng, X.** 2010. *Design and characterization of GRC-1: A soil for lunar terramechanics testing in Earth-ambient conditions.* Journal of Terramechanics, 47(6). pp. 361-377. 2010.

[5] http://www.humboldtmfg.com/c-1-p-43-id-1.html

[6] **Bekker, M. G.** 1960. *Off-the-road locomotion.* University of Michigan Press, Ann Arbor

[7] **D. R.Freitag, A. J. Green, K.-J. Melzer,** 1970. *Performance Evaluation Of Wheels For Lunar Vehicles (Summary Report).* U.S Army Engineer Waterways Experiment Station, Vicksburg, VA

[8] **Moreland, S., Skonieczny, K., Wettergreen, D., Asnani, V., Creager, C., Oravec, H.** 2011. *Inching Locomotion for Planetary Rover Mobility*. IEEE Aerospace Conference, Big Sky, MT.

BIOGRAPHIES

Scott Moreland *is a Ph.D. student in the Carnegie Mellon University Mechanical Engineering Department. Scott completed his bachelor's degree in mechanical engineering at the University of Toronto and a masters degree in mechanical engineering at Carnegie Mellon. Currently, the core of his research at the Robotics Institute addresses understanding the mobility performance of vehicles in planetary environments such as the Moon or Mars for the application of space exploration.*

Krzysztof Skonieczny *is a PhD candidate at the Carnegie Mellon University Robotics Institute, researching lunar mobility and excavation systems with the Field Robotics Center. He has Bachelor's and Master's degrees in aerospace engineering from the University of Toronto. He has worked with MDA Space Missions on operations and control for space robots including the Canadarm 2 (robotic arm for the International Space Station) and a prototype ExoMars rover (for the European Space Agency's flagship Mars mission). He also worked as an Operations Research analyst for the Canadian Department of National Defence, conducting field experiments of mobile ad hoc networks.*

Hiroaki Inotsume *is a M.E. candidate in the Department of Aerospace Engineering, Tohoku University, Japan. He received his bachelor's degree in Aerospace Engineering from Tohoku University in 2010. His research interests include the mobility analysis, mobility prediction, and motion planning/control for application to lunar and planetary exploration rovers. His current research is focusing on methods of traversing steep sandy slopes without significant slippage.*

Dr. David. S. Wettergreen *is a research professor at the Robotics Institute at Carnegie Mellon University. His research focuses on robotic exploration: underwater, on the surface, and in air and space, and in the necessary ingredients of perception, planning, learning and control for robot autonomy. His work spans conceptual and algorithm design through to field experimentation and results in mobile robots that explore the difficult, dangerous, and usually dirty places on Earth, in the service of scientific and technical investigations. Much of this work is relevant to ongoing and future space activities.*